Experimental evaluation on electrochemical corrosion of ion-implanted medium-carbon steel of titanium and titanium+nitrogen

F. Sanabria[a,*], L. Gil[b], C. Matos[b], E. D. V-Niño[a,c]

[a] Materials Science and Technology Research Group, Foundation of Researchers in Science and Technology of Materials, Bucaramanga, Colombia.
[b] Centro de Estudios de Corrosión y Biomateriales, Universidad Nacional Experimental Politécnica "Antonio José de Sucre", Puerto Ordaz, Venezuela.
[c] BCMaterials, Basque Center on Materials, Applications and Nanostructures, Leioa, Spain.

*Corresponding author, E-mail: foristom@gmail.com, phone: +57 304 637 8703

ABSTRACT
This paper proposes to evaluate and characterize the damage produced by electrochemical corrosion in AISI/SAE 1045 medium carbon steel surfaces, modified with titanium and titanium+nitrogen ions by three-dimensional ion implantation technique. By means of electrochemical tests such as linear polarization resistance, potentiodynamic polarization, and electrochemical impedance spectroscopy; it was quantified and compared the performance of non-implanted and implanted samples against electrochemical corrosion. From the results, it was found a considerable improvement in the performance of the surface-modified ferrous alloy in comparison with bare specimens. The degradation occurred after exposition in the saline environment was reduced up to 50% in terms of mass-loss or corrosion rates. Likewise, the inspection of the state and composition of AISI/SAE 1045 medium carbon steel microstructure, after the surface modification and chemical attack, by microscopy and spectroscopy characterization techniques, supported the findings in the electrochemical analysis and validated the favorable effect of the ion implantation technique as a method of protection against electrochemical corrosion, reducing the damage from the electrolyte and formation of corrosion products.

Keywords: AISI/SAE 1045 steel, Surface modification, Electrochemical characterization, Morphology, Surface engineering.

Evaluación experimental sobre corrosión electroquímica del acero de medio carbono implantado con iones de titanio y titanio+nitrógeno

RESUMEN
El presente trabajo trabajo de investigación se enfoca en evaluar y caracterizar el daño producido por la corrosión en superficies de acero de tipo AISI/SAE 1045 modificadas con iones de titanio y titanio+nitrógeno mediante la técnica de implantación iónica tridimensional; por medio de ensayos electroquímicos, como resistencia a polarización lineal, polarización potenciodinámica y espectroscopia de impedancia electroquímica, se cuantificó y comparó el comportamiento de la corrosión de sustratos no implantados e implantados. A partir de los resultados se encontró una mejora considerable en el rendimiento de la aleación ferrosa implantada en comparación con la no implantada, al reducir el daño producido por la corrosión en ambiente salino, hasta en un 50% en términos de corrosión o pérdida de masa. La inspección morfológica y composición de la superficie del acero de tipo AISI/SAE 1045, después de la modificación superficial y ataque químico, mediante técnicas de caracterización microscópica y espectroscópica, corroborraron los hallazgos obtenidos del análisis electroquímico y validaron el efecto favorable de la técnica de implantación iónica como método de protección contra la corrosión, reduciendo el daño del electrolito y la formación de productos de corrosión.

Palabras claves: Acero AISI/SAE 1045, Modificación superficial, Caracterización electroquímica, Morfología, Ingeniería de superficies.

INTRODUCTION

Structural materials such as low and medium carbon steel and stainless steel, broadly utilized in oil, gas, and transportation industry, are constantly exposed to both mechanical and chemical effects when they are in service. These interactions with such an aggressive media naturally promote surface reactions upon the uppermost region of the alloys, resulting mainly in interactions with such an

aggressive media, naturally promote surface reactions upon the uppermost region of the alloys resulting mainly in accelerated failures, loss of mass, changes in the chemical composition, and hence, promoting the degradation of the physical-chemical properties of structural components [1-5].

Corrosion, defined as "an irreversible interfacial reaction of a material (metal, ceramic, polymer) with its environment which results in the consumption of the material or in dissolution into the material of a component from the exposed environment" [6-8], represents one of the major problems of the modern industry. Its consequences, in global terms, can lead to economic losses where trillions of United States dollars (USD) are invested in order to mitigate the risk of damage in metal structures; safety issues with catastrophic failures in the transportation sector, where fatal tragedies have constantly been reported; and also environmental problems, where some discoveries have identified a harmful impact of both mass loss dissolved in consumable water streams and wasted material ending up in other environmental ecosystems [9-11].

For the above-mentioned reasons, current interdisciplinary studies in materials science, have had a certain interest in developing more innovative and advanced corrosion control technologies and also alternative cost reduction strategies, commonly focus on detection and prevention. Despite the diversity of existing technologies searching for minimizing the damage in alloys by corrosion, and being the later mostly a surface phenomenon, surface modification technologies such as ion implantation technique, provide an alternative solution for enhancing the physical-chemical properties of metallic materials. Several studies have achieved interesting results in the implantation process and its applications in ferrous alloys, demonstrating that it is possible to modify the structural and chemical composition of materials in order to improve its performance in typical aggressive media in engineering applications [12-20].

The objective of this work is to present a novel three-dimensional ion implantation (3DII) technique as an alternative surface modification method [21-26], where by means of high-voltage pulsed and electric arc discharges is generated enough energy to penetrate, simultaneously, metallic and non-metallic ionized particles into a solid; modifying both its surface microstructure and chemical composition in order to improve its corrosion resistance. After the surface modification in medium carbon steel, its performance against electrochemical corrosion in the saline environment was evaluated by electrochemical tests such as open circuit potential (OCP), linear polarization resistance (LPR), potentiodynamic polarization, and electrochemical impedance spectroscopy (EIS) techniques. Additionally, the state, morphology, and chemical composition of the surface microstructure was characterized by scanning electronic microscopy (SEM) and energy-dispersive X-ray spectroscopy (EDS).

METHODOLOGY

Sample preparation of low carbon steel AISI/SAE 1045 was carried out following the guidelines reported in ASTM E3-11 [27] and ASTM G1-03 [28] standards. The disk shape specimens whose diameter and width were 2.538 cm and 0.458 cm respectively were polished and grounded with silicon carbide paper from 80, 120, 240, 320, 400 down to 1200 until reaching a bright finishing. The surface texture was measured with a Taylor Hobson Precision unit, model Surtronic 25. Consecutively, coupons were chemically polished and cleaned with Nital (1% wt.) for 10 seconds prior to the metallographic analysis. The microstructure and grain size of the work material in question was determined by optical microscopy with the Nikon Eclipse TS100 microscope together with LECO IA-32 image processor software.

The surface modification of the substrates in AISI/SAE 1045 steel was carried out in the Joint Universal Plasma and Ion Technologies Experimental Reactor

(JUPITER) [16, 19, 23-26] by discharges hybrid of electric arc and high-voltage pulse (HVP) at low pressure with titanium (Ti) [2-4] and titanium+nitrogen (Ti+N) [5, 17] atmospheres. The surface treatment of the substrates was carried out for 10 min at an HVP applied of 10 kV, with a pulse duration of 0.25 ms and of frequency of 30 Hz. The pulverization of the titanium cathode was performed with an arc current of 140 A at a polarization potential of approximately 20 V. The pressure during the Ti and Ti+N treatment process was maintained at approximately 0.25 Pa and 1.00 Pa respectively. The substrates, before the surface treatment, were subjected to a sputtering process (generated with a pulsed electric discharge of 5 kV) in an argon atmosphere (Ar) for 15 minutes.

OCP measurements were run in order to establish the stability of the system in terms of electric potential according to the parameters and criteria indicated in ASTM C876-91 standard [29]; LPR, potentiodynamic polarization, and EIS was executed by following the guidance in ASTM G5-94 [30], ASTM G106-89 [31], ASTM G59-97 [32], ASTM G3-14 [33], and ASTM G102-89 [34] standards. Electrochemical tests were run by immersing the coupons in a typical glass made electrochemical cell which consists of a NaCl (3.5% wt.) solution acting as an electrolyte and three electrodes. The implanted AISI/SAE 1045 medium carbon steel specimens served as the working electrode with an area of 0.42 cm^2, two graphite rods as the counter electrode and a saturated calomel electrode as a reference electrode. The electrochemical cell was connected to a Gamry DCH2 potentiostat/galvanostat whose parameters were adjusted for each type of test. The corrosion rate (Vcorr) was obtained by the polarization resistance technique (Rp), with a scan rate of 7 mV/s, around the corrosion potential (Ecorr). The anodic and cathodic slopes were acquired from potentiodynamic polarization with a potential scan of 2 mV/s and potential range from -0.250 V to 1 V.

Data obtained by Gamry framework software, allowed to obtain the potentiodynamic curves and therefore, by extrapolating both the cathodic and anodic regions in the graphic, β_a, and β_c values, were respectively calculated. From β_a and β_c is estimated the corrosion current density (icorr) and then, with Equation 1, is determined the corrosion rate (CR) values for both implanted and non-implanted samples. Equation 1 is defined from Faraday's Law and involves AISI/SAE 1045 steel density, exposed area and equivalent weight.

$$CR = 0.1288 \frac{i_{corr}}{\rho A} \times EW, \qquad (1)$$

where CR in mpy, i_{corr} in μA, EW in gr/equivalent, ρ in gr/cm^3, and A in cm^2.

Microstructure analysis made upon non-implanted and implanted substrates with Ti and Ti+N ions was performed previously and later to the electrochemical test by optical microscopy with Nikon Eclipse TS100 optical microscope together with an image processor LECO IA-32. With the purpose of studying the state of the implanted surface and identifying the surface elemental composition after treatment. Surface morphology characterization was carried out by means of SEM-EDS, by implementing a FEI model Quanta 200 microscope.

RESULTS AND DISCUSSIONS

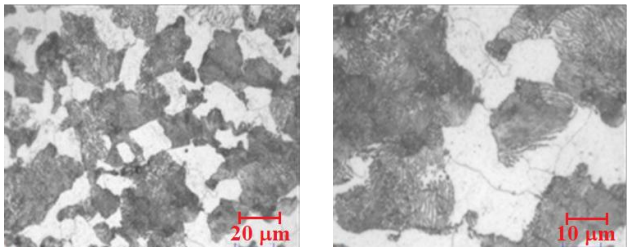
The results obtained from the surface characterizations and electrochemical tests were carried out to evaluate the effect of ion implantation on the medium carbon steel and also to identify changes upon the AISI/SAE 1045 medium carbon steel surface and its performance against electrochemical corrosion.

Steel characterization

Surface characterization of the material in question, prior surface modification was studied in order to get first sight of the microstructure morphology, identifying the

arrangement of present phases and verifying the microstructure of medium carbon steel.

Figure 1 shows the microstructure of non-implanted substrates at different magnifications obtained by optical microscopy. It is observed upon the surface an arrangement of perlite clusters (dim regions with an apparent high relief and laminar formation) distributed across a ferrite matrix (brighter zones) with a grain size No 7, according to ASTM E112-13 standard [35]. These results are in good agreement with the typical structure and phases distribution of AISI/SAE 1045 medium carbon steel [36].



(a) (b)

Fig. 1. AISI SAE 1045 microstructure. (a) 500X, and (b) 1000X.

With the purpose of identifying the effects that occurred upon the surface after the modification process and its likely influence upon corrosion resistance [37], an additional roughness test was performed comparing the surface texture between implanted and non-implanted samples. Table 1 presents the average roughness of the surfaces, identifying an increase in the magnitudes of implanted samples owing to the ion bombardment (Ar, N, Ti), deposition of foreign particles, particularly Ti and Ti+N species upon the steel surface.

Table 1. Roughness measurements.

Substrate	Roughness (µm)
Non-implanted	0.6 ± 0.04
Implanted with Ti ions	0.8 ± 0.06
Implanted with Ti+N ions	0.8 ± 0.04

Electrochemical characterization

The results obtained from the electrochemical tests OCP, LPR, potentiodynamic polarization, and EIS, determined the corrosion rates of AISI/SAE 1045 steel substrates non-implanted and implanted with ions of Ti and Ti+N.

OCP evaluation is a measurement that represents the thermodynamic tendency of metallic materials to corrode. That is the more negative potential values, the more its thermodynamic tendency to develop corrosion [7, 38]. In Figure 2 is observed that modified samples achieved the steady state in less time than non-implanted substrates, being the substrates implanted with Ti particles the ones with the best results in terms of stabilization, followed by a relative slight difference, the samples exposed to the hybrid treatment with Ti and N ions and finally the AISI/SAE 1045 samples without modifications.

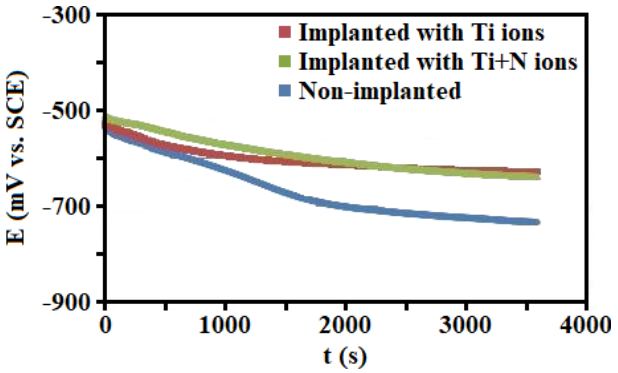


Fig. 2. OCP curves.

The values obtained in Table 2 presents these results, showing that samples implanted with Ti provided a more noble potential (−559 mV) than implanted samples with Ti+N (−578 mV) and non-implanted (−632 mV). At a first sight with the OCP results, is evident that the formation of Ti layers or surface enrichment with metallic particles, provides a better protection against electrochemical corrosion than other systems, by getting more noble the steel surface and therefore, delaying its corrosion tendency in saline environment. The changes of the surface microstructure, result of the ion implantation process, improved the nobility of the steel surface as the

hybrid treatment achieved better results than non-implanted as well, however in a minor degree than Ti implantation only. Farther potentiodynamic analysis had to be considered to validate these first outcomes.

Table 2. OCP results.

Substrate	Ecorr (mV)
Non-implanted	-632 ± 3
Implanted with Ti ions	-559 ± 1
Implanted with Ti+N ions	-578 ± 1

In order to obtain additional information concerning the corrosion resistance of AISI/SAE 1045, the quantitative assessment of the corrosion test was conducted by potentiodynamic polarization techniques. Figure 3 illustrates a comparison of the potentiodynamic polarization curves between implanted and nonimplanted samples exposed to NaCl (3.5% wt.) solution. Tafel extrapolation analysis was executed considering a range of ± 250 mV around the corrosion potential where eventually, the relevant parameters were estimated and listed in Table 3.

In Figure 3 it can be seen that the driving force (*i.e.* Ecorr) is more positive in implanted samples than non-implanted, which demonstrates a more passive behavior in the substrates implanted with Ti ions, than the implanted with Ti+N. This Ecorr validates the results obtained in OCP analysis in terms of corrosion tendency and it also provides a first approximation of the thermodynamic tendency after ion implantation; however, other parameters have to bear in mind when evaluating the corrosion kinetics.

The icorr is estimated by linear fit and Tafel extrapolation; from the potentiodynamic polarization results, it can be observed a direct correlation with the Vcorr defined by means of the Faraday's Law (Equation 1); that is, the greater the corrosion current density the bigger the reaction rates occurred upon the surface, and hence the greater the Vcorr. Therefore, since the icorr magnitudes reflect the dissolution rate through the passive layer, we can conclude that the samples modified by 3DII provide a protection mechanism against electrochemical corrosion in AISI/SAE 1045 medium carbon steel; where substrates implanted with Ti achieved the best corrosion resistance, followed by implanted with Ti+N.

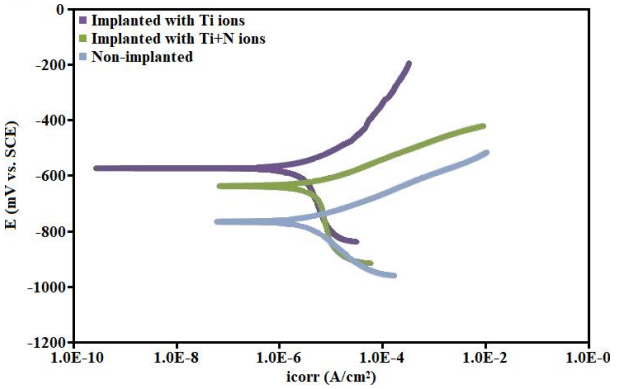


Fig. 3. Potentiodynamic polarization curves.

The results obtained in potentiodynamic polarization tests are validated by the LPR test, which is a non-destructive technique that allows determining the Rp by the relationship between the potential and the current (as an Ohm's law analogy). Table 4 reports the electrochemical parameters (Rp, icorr, and Vcorr) obtained from an analysis of the linear response of the current around the OCP applied on implanted and non-implanted substrates.

From LPR measurements it is observed an increase of the Rp magnitude in the implanted samples compared with the non-implanted substrate. The best resistive behavior was achieved by the samples implanted with Ti, followed by implanted with Ti+N, and the non-implanted. Despite offering better protection than non-implanted samples, it has been reported that the effect of nitrogen with titanium implanted upon ferrous alloys, promotes anodic reactions owing to the presence of unbonded nitrogen. That is, unbonded nitrogen atoms may accumulate at defect sites to form bubbles that are prone to burst and therefore expose the surface to the chemical attack, reducing the protective properties against corrosion [19, 39].

Table 3. Results obtained from potentiodynamic test.

Substrate	β_a (mV)	β_c (mV)	icorr (μA/cm^2)	Vcorr (mpy)	Ecorr (mV)
Non-implanted	7.21E-02	1.78E-01	8.10	3.71± 0.77	-767
Implanted with Ti ions	1.15E-01	7.51E-01	3.89	1.78± 0.78	-570
Implanted with Ti+N ions	7.29E-02	9.36E-01	5.69	2.61± 1.10	-636

Table 4. Results obtained from LPR test.

Substrate	Rp (Ω*cm^2)	icorr (μA/cm^2)	Vcorr (mpy)	Ecorr (mV)
Non-implanted	2162	12.31	5.64 ± 2.07	-744
Implanted with Ti ions	9252	4.68	2.14 ± 0.77	-579
Implanted with Ti+N ions	4245	10.33	4.74 ± 0.78	-662

In Nyquist plots, generally, the semicircle loop at high frequencies represents a capacitive behavior due to a corrosion process being controlled by charge transference, which means that when comparing several curves, an increment of the arc diameter represents a better resistive behavior (Figure 4). The deviation of the diameter in Nyquist arcs along the real axis is attributed to the series resistances involving the contact resistances with the electrolyte [40, 41]; the interpretation of these EIS parameters is described by the equivalent circuit (Figure 5).

In Figure 4, are illustrated the Nyquist curves for implanted samples exhibiting a larger diameter compared to the non-implanted curve, standing out the samples implanted with Ti, followed by the samples implanted with Ti+N; moreover, in samples implanted with Ti+N ions, a capacitive behavior is observed at high frequencies followed by an inductive behavior at low frequencies, which can be attributed to adsorbed species or dissolution processes of the corrosion products formed, to react with elements present on the metal surface and generate new products [41-45].

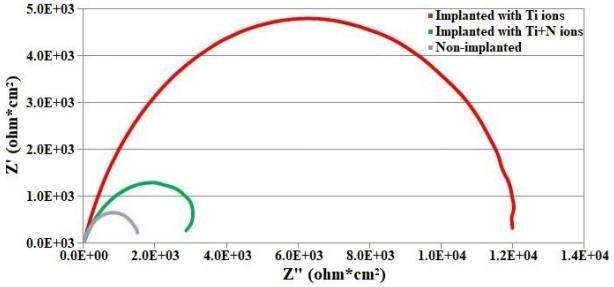


Fig. 4. Nyquist plots.

The equivalent circuit depicted in Figure 5 is modeled with the purpose of giving a physical interpretation of the corrosion mechanism developed in each sample and represented in the Nyquist results; this electrical circuit is widely used in studies of ion-selective membranes (or coated electrode-electrolyte interfaces) when examining metallic corrosion under coatings exposed to the corrosive environment [43-47]. Fitting parameters are estimated by Echem Analyst version 6.33 software and shown in Table 5.

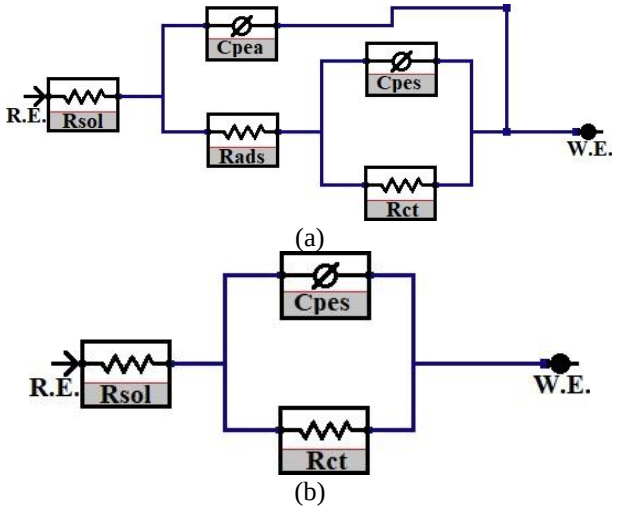


Fig. 5. Equivalent circuit Randles of order (a) II and (b) I.

In Figure 5(a) is represented the experimental data obtained from samples surface-modified, by means of an equivalent circuit Randles (of order II); it compromises an arrangement of electrical devices such as resistances and pseudo-capacitances or constant phase element (CPE) connected in series or parallel. The circuit integrates a first resistance, which represents the electrolyte resistance

(Rsol) simulating the ohmic behavior of the ion flux from the solution; a CPEa represents the implanted layer's capacitive response, acting as a dielectric in the implanted surface-electrolyte interface; a second resistance is the layer resistance (Rads), which reproduces an ohmic behavior as a part of the electrolyte pass through the porous surface of the formed layer until reaching the base material, that in touch with the electrolyte generates a second interface whose dielectric properties are represented by the second capacitance or electrochemistry double-layer capacitance (Cpes); this element is in parallel with the last resistance which acts as the charge transference resistance or polarization resistance (Rct). As non-implanted samples did not present a new film formation, a second model Randles (of order I) is proposed in Figure 5(b).

By comparing the implanted systems in Table 5, it can be seen that the layer resistance Rads was higher in samples implanted with Ti+N than the ones modified with Ti; these findings are likely due to the N implanted, which as mentioned before in the potentiodynamic tests, may promote anodic reactions yielding corrosion products that accumulated, act as a thicker barrier reducing the dissolution of the electrolyte.

On the other hand, due to CPE accounts for the deviation from ideal dielectric behavior and it is also related to the surface heterogeneity; and Rct values give a more approximate interpretation of the corrosion resistance; it is demonstrated that electrochemical characteristics of AISI/SAE 1045 have been affected by surface modification with 3DII, as well as performance in saline environments. Each ion implantation system has increased its Rct compared with the non-implanted, and therefore their resistance to charge transference, reaching the highest polarization resistance the samples implanted with Ti followed by the implanted with Ti+N. On the contrary, a decrease in CPE values indicated that the protective layer is either continuous or compact, being the samples implanted with Ti the ones that offered a better result compared with the samples implanted with Ti+N. Despite providing the lowest Rct, non-implanted AISI/SAE 1045 substrates unexpectedly demonstrated a better capacitive response which is probably owing to a thicker and homogeneous corrosion product layer.

Table 5. EIS data obtained by equivalent circuit simulation.

Parameter	Implanted with Ti ions	Implanted with Ti+N ions	Non-implanted
Rsol (ohm×cm^2)	1.05 E-01	1.14 E-01	2.88E+00
Cpea (S*Sa/cm^2)	3.75 E-06	1.16 E-04	-
n1	0.9	0.9	-
Rads (ohm×cm^2)	2.95 E+01	2.43 E+02	-
Cpes (S*Sa/cm^2)	6.37 E-05	2.56 E-04	1.05 E-05
n2	0.7	0.8	1.0
Rct (ohm×cm^2)	8.34 E+03	3.04 E+03	2.18 E+03
Goodness of Fit	1.71 E-02	2.07 E-02	4.05 E-03
Xi squared Kramers-Kronig	1.82 E-04	1.12 E-04	4.00 E-06

As for the n values, it represents the capacitive behavior (noticed in the Nyquist curves); when $n > 0.5$ the double electrochemical layer acts as a capacitor allowing the pass of charges from the electrolyte between interfaces (with formed layers and base material). The goodness of fit indicates the good approximation of the equivalent circuit and Kramers Kronig validates data [48-50]. By comparing the performance of implanted samples and the results in terms of polarization resistance, these results which in good agreement with other authors [17], it allows to conclude that 3DII provide a passive film whose determined thickness and density distributed superficially across the steel samples, which act as a surface barrier or blockage of the active sites of medium carbon steels when exposed to chemical attack. The relative improvement in

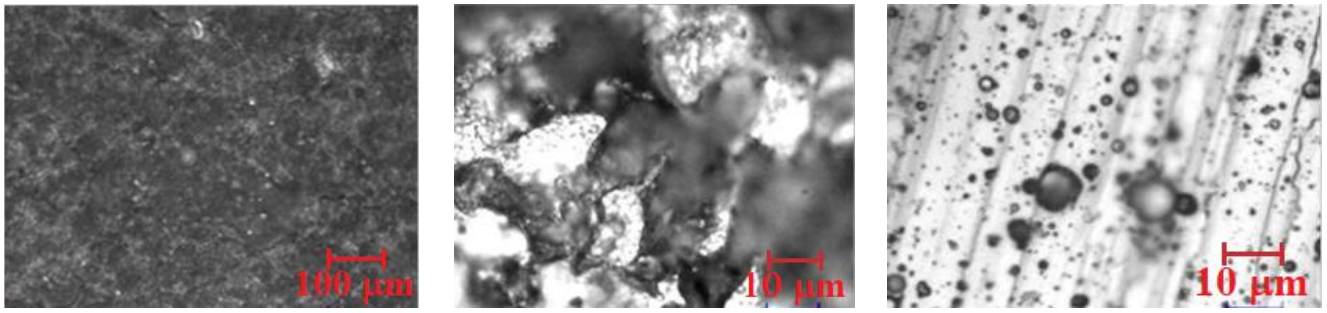
these values is also consistent with the findings in the potentiodynamic polarization experiments.

The EIS results also provide additional support to the effect produced by 3DII as a surface modification technique in metal alloys and an alternative solution to mitigate the damage by electrochemical corrosion; however, in order to reduce the corrosive activity, it is not unequivocal to determine which physical or chemical mechanism is occurring upon the surface vicinities of the material in question. From the findings in this paper, it may be suggested a significant role of surface roughness, as an increment in this property was identified after ion implantation. In the particular case of Ti+N implanted surfaces, it is possible that titanium nitride precipitation acts as a cathode and the steel matrix as an anode, promoting micro galvanic corrosion, and as a consequence, the surface of the substrate will preferentially corrode [51, 52].Some other works have suggested that ion implantation applied upon different alloys types, leads to the formation of complex mixture layers, improving the corrosion-resistant of the metal; in addition to this, the neutralizing reactions occurred upon the surfaces due to the chemical composition of formed films when in contact with the electrolyte, can minimize the reaction rates. Other works reported that the increment of defect density generated by the expansion of the lattice would reduce localized corrosion; and interestingly, the beneficial response of the radiation damage of certain materials, exposed to ion implantation was more evident than the chemical effect itself [7, 39, 40, 53, 54].

Morphology characterization

Optical inspection of implanted and non-implanted corroded surfaces was carried out in order to identify damage. In the micrograph shown in Figure 6(a), is observed a significant amount of corrosion products uniformly spread across the non-implanted surface. The damage gradually diminished in samples Ti+N treatment in Figure 6(b), where partial damage by action of the electrolyte is evident. In Figure 6(c), samples implanted with Ti demonstrated a better state with a relatively less surface deterioration. The deposited droplets whose size is between 1 μm and 10 μm, and distributed across the substrate surface, are due to the solidification of the evaporated material and the non-ionized Ti species (clusters formed during the evaporation of the Ti cathode) as well of the electric arc operation conditions in the JUPITER reactor [6, 17, 24].

The performance and superficial state of the substrates after the chemical attack are consistent with the previous electrochemical results, validating the beneficial effect of 3DII, as samples implanted with Ti and Ti+N provided better protection against corrosion with respect to the non-implanted surface.

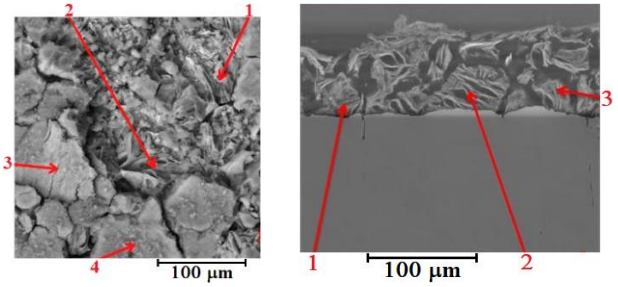


(a) (b) (c)

Fig. 6. Microscopic inspection of AISI/SAE 1045 substrates implanted after exposition in saline. (a) non-implanted; implanted with (b) Ti+N, and (c) Ti.

The inspections by SEM-EDS supported with more evidence and with elemental information in regard to the physical and chemical state of the implanted layer after exposition in saline solution. By the acquisition of cross-section and superficial images, were determined the thickness of the formed corrosion products and the elemental composition of different sections of interest

Figure 7(a) illustrates the typical damage of AISI/SAE 1045 when exposed to chloride solutions. Saline exposition caused the formation of a non-homogeneous and porous surface and a granular-like texture with cracks reaching sizes bigger than 100 µm. Cross-section micrograph in Figure 7(b) was identified as a porous corrosion products layer formed upon the surface, reaching a thickness of approximately 100 µm. The elemental composition identified the main alloy elements of the material in question together with a significant content of chlorine (Cl), oxygen (O), and sodium (Na) result of the saline exposition (Table 6).



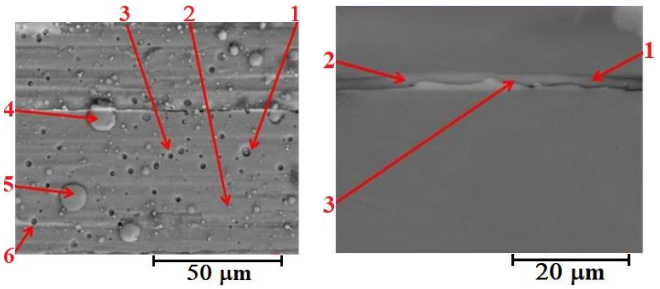
(a) (b)

Fig. 7. SEM micrographs: (a) surface and (b) cross-section of the non-implanted substrate after exposition to saline solution.

Table 6. Elemental analysis by EDS: (a) surface and (b) cross-section of the non-implanted substrate after corroded.

Element	Spectrum (wt. %)							
	Figure 7(a)					Figure 7(b)		
	1	2	3	5		1	2	3
Fe	74.52	72.57	65.67	47.48		35.60	39.38	57.08
C	-	-	-	-		51.77	46.44	13.37
O	19.15	18.23	27.09	18.32		10.49	12.41	25.08
Na	2.36	3.16	3.01	20.40		-	-	-
Al	-	-	-	-		0.39	0.43	0.65
Cl	3.21	4.82	2.99	12.69		0.52	0.70	2.44
Mn	0.76	1.21	1.24	1.11		1.23	0.64	1.38

Figure 8(a) shows the microstructure of the substrates implanted with Ti, where a heterogeneous morphology with porous of size between 2 µm – 10 µm that are distributed across the surface is identified. In addition to this, droplets produced by the electric arc discharge [17] are also deposited upon the surface with diameters between 2 µm and 15 µm. This effect is likely due to the enrichment of more noble species upon the surface achieved by the implantation process. Besides typical alloy elements of AISI/SAE 1045 medium carbon steel, as a result of the surface modification with Ti molecules, EDS results (Table 7) also demonstrated that droplets' chemical composition consisted mainly of Ti. In cross-section (Figure 8(b)) a corrosion products layer with an average of 0.5 µm was evidenced.



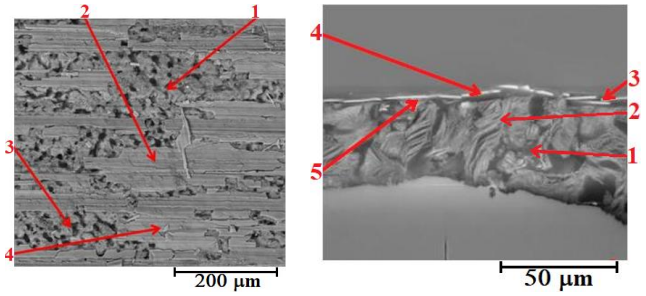
(a) (b)

Fig. 8. SEM micrographs: (a) surface and (b) cross-section of the substrate implanted with Ti after exposition to saline solution.

Table 7. Elemental analysis by EDS: (a) surface and (b) cross-section of the substrate implanted with Ti after corroded.

Element	Spectrum (wt. %)									
	Figure 8(a)							Figure 8(b)		
	1	2	3	4	5	6		1	2	3
Fe	68.00	20.73	40.62	1.57	2.96	54.86		12.00	19.44	22.63
C	17.30	10.70	12.07	6.34	5.72	6.90		40.60	34.32	36.92
O	-	-	-	-	-	-		11.25	10.50	7.75
Ti	14.70	68.57	47.31	92.09	91.32	38.24		36.15	35.74	32.70

Figure 9(a) shows the SEM micrograph of the Ti+N implanted surface, in which two surface textures can be distinguished: an upper laminar texture with a significant content of the implanted species (N and Ti), and an inner like porous texture with an appearance more deteriorated surface, the result of the loss material by the effect of the saline solution. The cross-section image (Figure 9(b)) showed a comparable thickness with that obtained in non-implanted samples, reaching a depth of approximately 60 μm; an apparent fragile interface is also identified in the uppermost of the surface. According to the EDS results (Table 8), it was detected the presence of Ti and N; these elements combined may increase the hardness of the surface and therefore making it more fragile and prone to crack or break, easing the penetration of the electrolyte into deeper layers and causing a negative impact on the corrosion resistance, as already evident in the electrochemical performance [4, 5].



(a) (b)

Fig. 9. SEM micrographs: (a) surface and (b) cross-section of the substrate implanted with Ti+N after exposition to saline solution.

Table 8. Elemental analysis by EDS: (a) surface and (b) cross-section of the substrate implanted with Ti+N after corroded.

Element	Spectrum (wt. %)								
	Figure 9(a)				Figure 9(b)				
	1	2	3	4	1	2	3	4	5
Fe	33.83	24.19	45.70	22.49	52.38	35.67	4.81	4.21	4.31
O	8.52	17.05	13.12	15.88	15.70	12.81	14.20	15.99	15.54
Na	10.18	5.61	3.69	6.32	-	-	-	-	-
Cl	8.08	5.52	4.09	8.16	-	-	-	-	-
Mn	0.65	0.56	0.91	0.67	0.44	1.27	-	-	-
Al	-	-	-	-	0.47	0.71	5.30	0.89	1.95
C	38.74	-	32.49	-	31.01	49.54	24.82	12.78	18.30
Ti	-	41.02	-	38.68	-	-	39.69	37.52	23.53
N	-	6.05	-	7.80	-	-	11.18	28.61	36.37

CONCLUSIONS

AISI/SAE 1045 medium carbon steel surfaces were modified with Ti and Ti+N ions respectively, by means of the 3DII technique, through hybrid discharges of electric arc and high voltage pulsed. As a result of these surfaces modification, it was obtained a surface roughness increment.

The potentiodynamic polarization and linear polarization resistance results confirmed the beneficial effect of the implanted samples with Ti and Ti+N by means of 3DII.

Substrates implanted with Ti and Ti+N ions, increased its corrosion potential, reducing its corrosion current density, and also increasing its polarization resistance in comparison with non-implanted substrates. These electrochemical parameters are correlated with the corrosion rates, being samples implanted with Ti, the treatment with the best corrosion rates hence corrosion resistance, followed by samples modified with Ti and N species.

The findings in the EIS analysis confirmed the potentiodynamic polarization results. Standing out samples implanted with Ti with a better corrosion resistance than Ti+N ion implantation and non-implanted. It was identified the corrosion mechanism occurred upon the implanted samples by equivalent circuits. The stability of the layer in the hybrid system was affected by the chemical combination of the implanted species. The fragility of the layer, product of an increment in the hardness achieved by the presence of Ti and N in the surface microstructure, produced a rupture of the superficial layer, promoting a rapid dissolution of the material as the aggressive electrolyte penetrated into inner layers.

Surface morphology and elemental analysis validated the superficial saturation of implanted species upon the surface by the presence of droplets with a high content of Ti. Damage by electrochemical corrosion was represented with corrosion products in all samples by the formation of a porous layer, with a significant thickness reduction in implanted coupons with Ti only and, in a minor degree, in samples implanted with Ti+N.

ACKNOWLEDGMENTS

The authors greatly acknowledge to the “Laboratorio de Física y Tecnología del Plasma y Corrosión, Universidad Industrial de Santander, Colombia” and to the “Centro de Investigación de la Siderúrgica del Orinoco, Venezuela”. This work was partially financed by the Colombian agency Colciencias through doctoral scholarship 617.

REFERENCIAS

[1] Salazar-Jiménez, J. A. (2015) “Introducción al fenómeno de corrosión: tipos, factores que influyen y control para la protección de materiales (Nota técnica)”. *Tecnología en Marcha* 28(3):127-136.

[2] V-Niño, E. D., Garnica, H., Dugar-Zhabon, V., Castillo, G. (2014) “Behavior of AISI SAE 1020 steel implanted by titanium and exposed to bacteria sulphate deoxidizer”. *Journal of Physics: Conference Series* 511(012080):1-5, doi: 10.1088/1742-6596/511/1/012080.

[3] Valbuena Niño, E. D., Peña Ballesteros, D. Y., Reyes Corzo, M. S., Dugar-Zhabon V. (2013) “Estudio experimental de la resistencia a la corrosión de un acero al carbono AISI-SAE 1020 implantado con iones de titanio”. *Revista Latinoamericana de Metalurgia y Materiales* 33(1):138-146.

[4] Valbuena Niño, E. D., Garnica, H., Dugar-Zhabon, V. D., Herrera Súarez, J. L. (2012) “Determinación de la velocidad de corrosión de aceros AISI SAE 1010, 1020, 1045 implantados con iones Ti”. *Revista Tumbaga* 1(7):37-45.

[5] Valbuena Niño, E. D., Salinas, D. V., Peña, D. Y., Chinchilla, L. F. (2011) “Modificación superficial de un acero AISI SAE 1045 mediante la implantación de iones de nitrógeno y titanio”. *Iteckne* 8(1):31-36, doi: 10.15332/iteckne.v8i1.259.

[6] Guo, J., Yang, S., Shang, C., Wang, Y., He, X. (2008) “Influence of carbon content and microstructure on corrosion behaviour of low alloy steels in a Cl-containing environment”. *Corrosion Science* 51(2):242–251, doi: 10.1016/j.corsci.2008.10.025.

[7] Padhy, N., Ningshen, S., Panigrahi, B. K., Kamachi Mudali, U. (2010) “Corrosion behaviour of nitrogen ion implanted AISI type 304L stainless steel in nitric acid medium”. *Corrosion Science* 52(1):104–112, doi: 10.1016/j.corsci.2009.08.042.

[8] Ma, Y., Li, Y., Wang, F. (2010) "The atmospheric corrosion kinetics of low carbon steel in a tropical marine environment". *Corrosion Science* 52(5):1796–1800, doi: 10.1016/j.corsci.2010.01.022.

[9] Gao, K., Li, D., Pang, X., Yang, S. (2010) "Corrosion behaviour of low-carbon bainitic steel under a constant elastic load". *Corrosion Science* 52(10):3428-3434, doi: 10.1016/j.corsci.2010.06.021.

[10] Hoog, N.A., Mayer, M. J. J., Miedema, H., Wagterveld, R. M., Saakes, M., Olthuis, W., van den Berg, A. (2014) "Stub resonators for online monitoring early stages of corrosion". *Sensors and Actuators B: Chemical* 202:1117-1136, doi: 10.1016/j.snb.2014.06.026.

[11] Bai, P., Zhao, H., Zheng, S., Chen, C. (2015) "Initiation and developmental stages of steel corrosion in wet H2S environments". *Corrosion Science* 93:109-119, doi: 10.1016/j.corsci.2015.01.024.

[12] Dearnaley, G. (1969) "Ion bombardment and implantation". *Reports on Progress in Physics* 32:405-491.

[13] Radjabov, T. D. (1988) "Improvement of the corrosión properties of metals by ion implantation". *Vacuum* 38(11):979-985, doi: 10.1016/0042-207X(88)90558-1.

[14] Mccafferty, E. (2001) "Effect of ion implantation on the corrosion behavior of iron, stainless steels, and aluminum-A review". *Corrosion* 57(12):1011-1029, doi: 10.5006/1.3281675.

[15] Jothi, K., Palanivelu, K. (2016) "Praseodymium oxide modified hybrid silane coatings for anticorrosión applications". *Surface Engineering* 32(1):47-52, doi: 10.1179/1743294414Y.0000000333.

[16] Parada-Becerra, F., Cabanzo, R., Dugar-Zhabon, V., Tsygankov, P., Mejia-Ospino, E., V-Niño, E. D. (2012) "Plasma temperature measurement in a hybrid discharge by using optical diagnostics". *Journal of Physics: Conference Series* 370(012054):1-6, doi: 10.1088/1742-6596/370/1/012054.

[17] Valbuena-Niño, E. D., Gil, L., Hernández-Molina, L., Barba-Ortega, J. J., Dugar-Zhabon, V. (2016) "Characterization of the low alloy steel modified superficially with ions of titanium and nitrogen". *CT&F - Ciencia, Tecnología y Futuro* 6(3):127-138.

[18] Sanabria, F., Viejo, F., V-Niño, E. D. (2019) "Performance in saline environment of a carbon steel surface modified by three dimensional ion implantation". *Journal of Physics: Conference Series* 1403(012015):1-7, doi: 10.1088/1742-6596/1403/1/012015.

[19] Valbuena-Niño, E. D., Gil, L., Hernández, L., Sanabria, F. (2020) "Corrosion resistance of a carbon-steel surface modified by three-dimensional ion implantation and electric arc". *Advances in Materials Research* 9(1):1-14, doi: 10.12989/amr.2020.9.1.001.

[20] Sanabria-Martínez, F., Valbuena-Niño, E. D., Rincón-Joya, M., Estupiñán-Duran, H. A., Viejo-Abrante, F. (2020) "Surface evaluation of carbon steel doped with nitrogen ions". *Rev. UIS Ing*. 19(1):205-212, doi: 10.18273/revuin.v19n1-2020019.

[21] Khvesyuk, V. I., Tsygankov, P. A. (1997) "The use of a highvoltage discharge at low pressure for 3D ion implantation". *Surface and Coatings Technology* 96(1):68-74, doi: 10.1016/S0257-8972(97)00117-5.

[22] Dougar-Jabon, V. D., Dulce-Moreno, J., Tsygankov, P. A. (2002) "High voltage pulse discharge for ion treatment of metals". *Review of Scientific Instruments* 73(2):828-830, doi: 10.1063/1.1429785.

[23] Dulce-Moreno, H. J., Tsygankov, P. A., Dugar-Zhabon, V., V-Niño, E. D., Parada, F. F. (2011) "Estudio de los haces electrónicos en la descarga eléctrica de alto voltaje a bajas presiones". *Puente Revista Científica* 5(2):21-26, doi: 10.18566/puente.v5n2.a03.

[24] Tsygankov, P., Plata, A., V-Niño, E. D., Ochoa, C., Parada, F., Chacón, C., Dugar-Zhabon, V. (2011) "Estudio de características voltio-ampéricas y peculiaridades de funcionamiento de un vaporizador de arco en vacío". *Revista Colombiana de Física* 43(2):458-462.

[25] Dugar-Zhabon, V. D., Dulcé-Moreno, H. J., Garnica-Villamizar, H. A., Valbuena-Niño, E. D. (2012) "A new method for surface modifications of carbon steels and alloys". *Materials Research* 15(6):969-973, doi: 10.1590/S1516-14392012005000133.

[26] Valbuena Niño, E. D., Dugar-zhabon, V., Dulce Moreno, H. J., Peña Rodríguez, G., Garnica, H. A., Tsygankov, P. (2012) "Aplicación de descargas simultáneas de alto voltaje y arco eléctrico para el tratamiento superficial avanzado de metales". *Iteckne* 9(1):14-20, doi: 10.15332/iteckne.v9i1.56.

[27] American Society of Testing Materials (2011) "*Standard guide for preparation of metallographic specimens, ASTM E3-11*" West Conshohocken, U.S.A., American Society for Testing Materials (ASTM).

[28] American Society for Testing Materials (2011) "*Standard practice for preparing, cleaning, and evaluating corrosion test specimens, ASTM G1-03*" West Conshohocken, U.S.A., American Society for Testing Materials (ASTM).

[29] American Society of Testing Materials (1999) "*Standard test method for half-cell potentials of uncoated reinforcing steel in concrete, ASTM C876-91*" West Conshohocken, U.S.A., American Society for Testing Materials (ASTM).

[30] American Society of Testing Materials (2011) "*Standard reference test method for making potentiostatic and potenciodynamic anodic polarization measurements, ASTM G5-94*" West Conshohocken, U.S.A., American Society for Testing Materials (ASTM).

[31] American Society of Testing Materials (2015) "*Standard practice for verification of algorithm and equipment for electrochemical impedance measurements, ASTM G106-89*" West Conshohocken, U.S.A., American Society for Testing Materials (ASTM).

[32] American Society of Testing Materials (2014) "*Standard test method for conducting potentiodynamic polarization resistance measurements, ASTM G59–97*" West Conshohocken, U.S.A., American Society for Testing Materials (ASTM).

[33] American Society of Testing Materials (2019) "*Standard practice for conventions applicable to electrochemical measurements in corrosion testing, ASTM G3-14*" West Conshohocken, U.S.A., American Society for Testing Materials (ASTM).

[34] American Society of Testing Materials (2015) "*Standard practice for calculation of corrosion rates and related information from electrochemical measurements, ASTM G102-89*" West Conshohocken, U.S.A., American Society for Testing Materials (ASTM).

[35] American Society of Testing Materials (2013) "*Standard test methods for determining average grain size, ASTM E112-13*" West Conshohocken, U.S.A., American Society for Testing Materials (ASTM).

[36] Kadowaki, M., Muto, I., Katayama, H., Masuda, H., Sugawara, Y., Hara, N. (2019) "Effectiveness of an intercritical heat-treatment on localized corrosion resistance at the microstructural boundaries of medium-carbon steels". *Corrosion Science* 154:159-177, doi: 10.1016/j.corsci.2019.04.019.

[37] Martínez Gutiérrez, J., Lluveras Pérez, E., Marrero Águila, R. (2019) "Comportamiento de la rugosidad superficial del acero luego de exposición natural en exterior e interior". *Revista U.D.C.A Actualidad & Divulgación Científica* 22(1):1-10, doi: 10.31910/rudca.v22.n1.2019.1193.

[38] Maleki-Ghaleh, H., Khalil-Allafi, J., Sadeghpour-Motlagh, M., Shakeri, M. S., Masoudfar, S., Farrokhi, A., Beygi Khosrowshahi, Y., Nadernezhad, A., Siadati, M. H., Javidi, M., Shakiba, M., Aghaie, E. (2014) "Effect of surface modification by nitrogen ion implantation on the electrochemical and cellular behaviors of super-elastic NiTi shape memory alloy". *Journal of Materials Science: Materials in Medicine* 25:2605-2617, doi: 10.1007/s10856-014-5283-4.

[39] Vigen Karimi, M., Sinha, S. K., Kothari, D. C., Khanna, A. K., Tyagi, A. K. (2002) "Effect of ion implantation on corrosion resistance and high temperature oxidation resistance of Ti deposited 316 stainless steel". *Surface and Coatings Technology* 158-159:609-614, doi: 10.1016/S0257-8972(02)00319-5.

[40] Anandan, C., William Grips, V. K., Ezhil Selvi, V., Rajam, K. S. (2007) "Electrochemical studies of stainless steel implanted with nitrogen and oxygen by plasma immersion ion implantation". *Surface and Coatings Technology* 201(18):7873-7879, doi: 10.1016/j.surfcoat.2007.03.034.

[41] Cabrera-Sierra, R., Marín-Cruz, J., González, I. (2007) "La utilización de la espectroscopia de impedancia electroquímica (EIS) para identificar diferentes estados superficiales en el proceso de corrosión del acero al carbono en medios amargos". *Bol. Soc. Quím. Méx.* 1(1):32-41.

[42] Pereira, C., De Souza, F. S., Marin, G., Hickel, S. M., Bindera, C., Nelmo, A. (2017) "Corrosion resistance of low-carbon steel modified by plasma nitriding and diamond-like carbon". *Diamond & Related Materials* 80:54-161, doi: 10.1016/j.diamond.2017.11.001.

[43] Jimenez-Morales, A., Galvan, J. C., Rodriguez, R., De Dambo-renea, J. J. (1997) "Electrochemical study of the corrosion behavior of copper surfaces modified by nitrogen ion implantation". *Journal of Applied Electrochemistry* 27:550-557, doi: 10.1023/A:1018446628256.

[44] Piratoba Morales, U., Vera López, E., Ortiz Otálora, C. (2010) "Aspectos básicos en la interpretación de diagramas de impedancia electroquímica". *DYNA* 77(162):13-19.

[45] Piratoba Morales, U., Mariño Camargo, A., Olaya Flórez, J. J. (2010) "Impedancia electroquímica - Interpretación de diagramas típicos con circuitos equivalentes". *DYNA* 77(164):69-75.

[46] Olaya, J. J., Piratoba, U., Rodil, S. E. (2011) "Resistencia a la corrosión de recubrimientos de CRN depositados por PVD con UBM: Tecnología eficiente y ambientalmente limpia". *Revista Latinoamericana de Metalurgia y Materiales* 31(1):44-51.

[47] Abdi, F., Savaloni, H. (2017) "Surface nanostructure modification of Al substrates by N+ ion implantation and their corrosion inhibition". *Transactions of Nonferrous Metals Society of Chin*a 27(3):701-710, doi: 10.1016/S1003-6326(17)60078-5.

[48] Sadkowski, A. (2004) "CNLS fits and Kramers–Kronig validation of resonant EIS data". *Journal of Electroanalytical Chemistry* 573:241–253, doi: 10.1016/j.jelechem.2004.07.009.

[49] Baboian, R. (2005) "*Corrosion test and standards: Application and interpretation, 2nd edition*" West Conshohocken, U.S.A., American Society for Testing Materials (ASTM).

[50] Liu, C., Bi, Q., Leyland, A., Matthews, A. (2003) "An electrochemical impedance spectroscopy study of the corrosion behaviour of PVD coated steels in 0.5 N NaCl aqueous solution: Part II. EIS interpretation of corrosion behaviour". *Corrosion Science* 45(6):1257-1273, doi: 10.1016/S0010-938X(02)00214-7.

[51] Chang, M., Su, J., Hu, G., Zhai, B., Meng, D., Sun, L., Chen, Y., Li, Y., Cui, Y. (2016) "Enhancement of corrosion resistance of a biomedical grade NiTi shape memory alloy by cyclic potentiodynamic polarization in PBS solution". *Int. J. Electrochem. Sci.* 11:1092-1098.

[52] Vasilescu, C., Drob, S. I., Calderon Moreno, J. M., Osiceanu, P., Popa, M., Vasilescu, E., Marcu, M., Drob, P. (2015) "Long-term corrosion resistance of new Ti-Ta-Zr alloy in simulated physiological fluids by electrochemical and surface analysis methods". *Corrosion Science* 93:310-323, doi: 10.1016/j.corsci.2015.01.038.

[53] Muthukumaran, V., Selladura, V., Nandhakumar, S., Senthilkumar, M. (2010) "Experimental investigation on corrosion and hardness of ion implanted AISI 316L stainless steel". *Materials and Design* 31:2813-2817, doi: 10.1016/j.matdes.2010.01.007.

[54] Fossati, A., Borgioli, F., Galvanetto, E., Bacci, T. (2006) "Glow-discharge nitriding of AISI 316L austenitic stainless steel: influence of treatment time". *Surface and Coatings Technology* 200(11):3511-3517, doi: 10.1016/j.surfcoat.2004.10.122.